IOPscience iopscience.iop.org

Home Search Collections Journals About Contact us My IOPscience

A self-consistent embedding approach to the electronic structure of random systems

This article has been downloaded from IOPscience. Please scroll down to see the full text article.

1989 J. Phys.: Condens. Matter 1 509

(http://iopscience.iop.org/0953-8984/1/3/002)

View the table of contents for this issue, or go to the journal homepage for more

Download details:
IP Address: 171.66.16.90
The article was downloaded on 10/05/2010 at 16:59

Please note that terms and conditions apply.

J. Phys.: Condens. Matter 1 (1989) 509–518. Printed in the UK

A self-consistent embedding approach to the electronic structure of random systems

Abhijit Mookerjee and Samita Bardhan
Department of Physics, Indian Institute of Technology, Kanpur 208016, India

Received 4 May 1988

Abstract. On the basis of the partition theorem and the embedding ideas of Inglesfield, we develop a methodology to study the electronic structure of random systems. The equations for the Green functions are confined to a finite-cluster region and the influence of the rest of the region appears as a surface potential. The herglotz properties are satisfied in the approximation. We illustrate the methodology by applying it to a binary distribution of spherically symmetric wells in a coherent jellium. This is the alloy generalisation of the impurity work of Inglesfield referred to in the text.

1. Introduction

One of the most powerful techniques available these days to study the electronic structure of random alloys is the coherent potential approximation (CPA). The scheme has been extensively applied in both the tight-binding and the Korringa–Kohn–Rostoker (KKR) scattering approaches. Increasingly, as one wants to make realistic quantitative calculations, it is being felt that the single-site or single-muffin-tin approximation appears to be inadequate in a large class of systems. The effects of clustering, short-range order, lattice relaxation and similar local environmental effects need to be effectively tackled. Self-consistent analyticity-preserving cluster CPAs have been proposed, in both the tight-binding (Mookerjee 1973, Kumar *et al* 1982, Gray and Kaplan 1976a, b) and the KKR approaches (Gonis *et al* 1984, Mookerjee 1987). In this paper, we wish to propose an approach for developing a CPA encompassing both single-potential wells and clusters of wells. The methodology is an extension to random systems of the embedding technique introduced by Inglesfield (1971, 1972, 1981) for impurities and surfaces.

Inglesfield's idea is based on the fact that the solutions of second-order elliptic differential equations (such as the Schrödinger equation) in all space may be solved by confining ourselves to a finite closed subspace. The effect of the remaining space is incorporated in the effective Hamiltonian as a surface potential.

In comparison, the philosophy behind all CPAs may be summarised in the following steps.

(i) We first divide the space into two subspaces I and II. In I, we treat the potential *exactly* while, in II, we replace the random potential by an effective periodic energy-dependent coherent potential.

0953-8984/89/030509 + 10 $02.50 © 1989 IOP Publishing Ltd

(ii) We then determine the Green function for this system for different realisations of the random potential in I. This Green function averaged over different realisations is then equated to the Green function of a system where the effective, coherent potential replaces the exact potential in *all space*. This determines the coherent potential.

Region I could be a single-muffin-tin potential, a cluster of potentials, or a cluster with a modified spherical boundary (Inglesfield 1981) as in figure 5 (see later). Within I, therefore, clustering short-range order or lattice relaxation effects may be incorporated. The exact potential $V(\boldsymbol{r})$ in this region has a random configuration C with appropriate probability densities $P(V)D(V)$.

In region II, we assume that we know the exact solution

$$[-\tfrac{1}{2}\nabla^2 + U(\boldsymbol{r})]\psi(\boldsymbol{r}) = E\psi(\boldsymbol{r}). \tag{1.1}$$

From this we construct a Green function $g(\boldsymbol{r}, \boldsymbol{r}', U)$ satisfying

$$[-\tfrac{1}{2}\nabla^2 + U(\boldsymbol{r}) - E]g(\boldsymbol{r}, \boldsymbol{r}', U) = \delta(\boldsymbol{r} - \boldsymbol{r}') \tag{1.2}$$

and the boundary condition $\partial g/\partial n_S = 0$ on the surface S between the two regions I and II. $\partial/\partial n_S$ denotes the derivative normal to the surface S. Now from equations (1.1) and (1.2), using the Green theorem and the boundary conditions on S, we obtain

$$\psi(\boldsymbol{r}) = -\tfrac{1}{2}\int_S \mathrm{d}^2 r_S \, g(\boldsymbol{r}, \boldsymbol{r}_S, U) \left.\frac{\partial \psi}{\partial n_S}\right|_{r=r_S}.$$

If we now introduce the functional inverse $k(\boldsymbol{r}, \boldsymbol{r}', U)$ of the Green function defined in equation (1.2), we may invert this integral equation

$$\frac{\partial \psi(\boldsymbol{r}_S)}{\partial n_S} = -2\int_S \mathrm{d}^2 r'_S \, k(\boldsymbol{r}_S, \boldsymbol{r}'_S, U)\varphi(\boldsymbol{r}'_S). \tag{1.3}$$

Let us now introduce the trial wavefunction Φ in all space, which takes the value $\psi(\boldsymbol{r})$ in II and a trial function $\varphi(\boldsymbol{r})$ in I, with $\varphi(\boldsymbol{r}) = \psi(\boldsymbol{r})$ on S. If we now vary Φ in equation (1.1) but still match Φ and ψ on S, we obtain

$$\int_{\mathrm{II}} \mathrm{d}^3 \boldsymbol{r} \, |\psi(\boldsymbol{r})|^2 = -\int_S \mathrm{d}^2 r_S \int_S \mathrm{d}^2 r'_S \, \varphi(\boldsymbol{r}_S) \frac{\partial}{\partial E}[k(\boldsymbol{r}_S, \boldsymbol{r}'_S, E)]\varphi(\boldsymbol{r}'_S). \tag{1.4}$$

The next step involves the calculation of the energy E as $[\int \mathrm{d}^3 \boldsymbol{r} \, \Phi^*(\boldsymbol{r})\boldsymbol{H}\Phi(\boldsymbol{r})/\int \mathrm{d}^3 \boldsymbol{r} \, \Phi^*(\boldsymbol{r})\Phi(\boldsymbol{r})]$ and using equations (1.3) and (1.4) to replace the terms involving ψ in II. This procedure is identical with that of Inglesfield and the reader is referred to that work for the algebraic details. A variational minimisation of E with respect to the trial function φ in I and an evaluation of the kernel $k(\boldsymbol{r}, \boldsymbol{r}', U)$ at the exact energy E of the total system yields the effective Schrödinger equation

$$\left[-\tfrac{1}{2}\nabla^2 + \tfrac{1}{2}\delta(\boldsymbol{r} - \boldsymbol{r}_S)\frac{\partial}{\partial n_S} + U(\boldsymbol{r})\right]\varphi(\boldsymbol{r}) + \delta(\boldsymbol{r} - \boldsymbol{r}_S)\int_S \mathrm{d}^2 r_S \, k(\boldsymbol{r}_S, \boldsymbol{r}'_S, U)\varphi(\boldsymbol{r}'_S) = E\varphi(\boldsymbol{r})$$

with

$$\boldsymbol{r} \in \mathrm{I}. \tag{1.5}$$

Note that this effective Schrödinger equation acts on the space I *alone*. The effect of the space II appears as the *surface potential* operator $\boldsymbol{K}(E, U) = \delta(\boldsymbol{r} - \boldsymbol{r}_S)\int \mathrm{d}^3 \boldsymbol{r}'_S \, k(\boldsymbol{r}_S, \boldsymbol{r}'_S, U)$. The term $\frac{1}{2}\delta(\boldsymbol{r} - \boldsymbol{r}_S)(\partial/\partial n_S)$ ensures that the effective Hamiltonian remains Hermitian

in region I alone. Usually region I is a small subspace, so that equation (1.5) is a significant simplification, provided that we can determine the kernel $\boldsymbol{K}(E, U)$ on the surface S with ease. Effectively, we have partitioned the space, and within the tight-binding (or any countable basis) approach this is exactly the *partition theorem* (Kumar *et al* 1982) used to introduce the cluster coherent potential approximation (CCPA).

Our basic approximation now involves replacing the random potential $U(\boldsymbol{r})$ in II by an energy-dependent coherent potential $u(\boldsymbol{r}, E)$ which is *invariant* under lattice translations $u(\boldsymbol{r}+\boldsymbol{R}, E) = u(\boldsymbol{r}, E)$, where $\boldsymbol{R}$ is a lattice vector. Using equation (1.5), we obtain the Green function for the whole space

$$[E\boldsymbol{I} - \boldsymbol{H}(V) + \boldsymbol{K}(E, u)]\boldsymbol{G}(V, u, E) = \boldsymbol{I}. \tag{1.6}$$

The self-consistent equation for the coherent potential u is then

$$\int D(V)P(V)G(\boldsymbol{r}, \boldsymbol{r}', E, V, u) = G(\boldsymbol{r}, \boldsymbol{r}', E, u, u) \tag{1.7}$$

with *both* $\boldsymbol{r}, \boldsymbol{r}'$ in I. This is the basic CCPA equation. The choice of region I incorporates the cluster effects.

The construction of the surface potential involves the calculation of the Green function in II with the additional boundary condition that its normal derivative vanishes on the boundary S. We shall illustrate this by two examples.

From equation (1.6), we note that the Hamiltonian $\boldsymbol{H}(V)$ in the subspace I is Hermitian; moreover the 'surface potential' $\boldsymbol{K}(E, u)$ is herglotz provided that the Green function $g(\boldsymbol{r}, \boldsymbol{r}', u)$ defined in equation (1.2) is herglotz. This condition is sufficient to ensure the herglotz nature of $\boldsymbol{G}(V, u, E)$ for each realisation of V. Equation (1.7) then ensures that the averaged $G(\boldsymbol{r}, \boldsymbol{r}', E, u, u)$ is also herglotz. In the applications which follow, to ensure the herglotz property of the averaged Green function, we have to ensure that the Green function in the truncated space II is constructed to be herglotz. We have done so for the numerical examples involving the coherent jellium.

1.1. The coherent jellium

This assumes that the coherent potential is independent of $\boldsymbol{r}$ in II: $u(\boldsymbol{r}, E) = u(E)$. Then we have

$$g(\boldsymbol{r}, \boldsymbol{r}', u) = -\frac{\mathrm{i}k}{4\pi}\sum_L \left(j_l(kr_<) - \frac{j_l'(kr_S)}{h_l'(kr_S)}h_l(kr_<)\right)h_l(kr_>)Y_L(\hat{r})Y_L(\hat{r}') \tag{1.8}$$

where $k = [(2m/\hbar^2)(u-E)]^{1/2}$.

It is easy to check that the boundary condition is obeyed on S. On S, we have

$$g(\boldsymbol{r}_S, \boldsymbol{r}_S', U) = -\frac{\mathrm{i}k}{4\pi}\sum_L W(j_l, h_l)\frac{h_l(kr_S)}{h_l'(kr_S)}Y_L(\hat{r})Y_L(\hat{r}') = \sum_L g_l(kr_S)Y_L(\hat{r})Y_L(\hat{r}'). \tag{1.9a}$$

Since the Wronskian $W(j_l, h_l) = 1/k^2r_S^2$, we have

$$g_l(kr_S) = (-\mathrm{i}/4\pi kr_S^2)[h_l(kr_S)/h_l'(kr_S)]. \tag{1.9b}$$

From the above, it follows that, if

$$k(\boldsymbol{r}_S, \boldsymbol{r}_S', U) = \Sigma_L k_l(kr_S)Y_L(\hat{r})Y_L(\hat{r}')$$

then $r_S^4 k_l(kr_S)g_l(kr_S) = 1$ (see Appendix).

For states with s symmetry, $l = 0$ and $m = 0$; for the flat potential we have $h_0(kr_s) = \exp(ikr_s)/ikr_s$ so that $k_0(kr_s) = (1 - ikr_s)/4\pi r_s^3$. This is Inglesfield's result for the s Green function for the flat three-dimensional well.

1.2. The coherent crystal

In case we wish to represent the region II by a crystalline array of coherent muffin-tin potentials, we may generalise the Green function expressions given by Faulkner and Stocks (1980). Our aim is to generate a Green function whose derivative vanishes at the boundary S of region I. In the usual KKR calculations the Green function with this boundary condition is usually not encountered. We shall first illustrate this by a simple example when region I has a single muffin-tin potential centred at $\boldsymbol{R}_n$. Let $J_l(\boldsymbol{r}, E)$ and $H_l(\boldsymbol{r}, E)$ be the regular and irregular solutions at the origin of the muffin tin potential:

$$-(1/r_n^2)(\mathrm{d}^2/\mathrm{d}r_n^2)(r_n Z_l) + [U(r_n) + l(l+1)/r_n^2 - E]Z_l = 0 \qquad \boldsymbol{r}_n = \boldsymbol{r} - \boldsymbol{R}_n.$$

$J_l(r, E)$ smoothly joins onto $j_l(kr)c_l^n - ikh_l(kr)$ when $r > r_M$, the radius of the muffin-tin sphere, while $H_l(r, E)$ joins smoothly onto $j_l(kr)$ for $r > r_M$. $c_l^n \delta_{LL'}$ is the inverse of the scattering **t**-matrix associated with the nth muffin-tin potential.

$$g(\boldsymbol{r}, \boldsymbol{r}', U) = C \sum_{LL'} \sum \left(J_l(r_<, E) - \frac{J_l'(r_{ns})}{H_l'(r_{ns})} H_l(r_<, E) \right) Q_{LL}^{nn}(r_>, E) Y_L(\hat{\boldsymbol{r}}) Y_{L'}(\hat{\boldsymbol{r}}')$$

$$Q_{LL'}^{nm}(r, E) = T_{LL'}^{nm}(E) J_l(r, E) - \delta_{LL'} \delta_{nm} H_l(r, E). \tag{1.10}$$

$T_{LL'}^{nm}(E)$ is the path operator $\mathbf{T} = (\mathbf{c} - \mathbf{B})^{-1}$ where $c_{LL'}^{nm} = c_L^n \delta_{nm} \delta_{LL'}$ is the inverse **t**-matrix and $B_{LL'}^{nm}$ is the structure factor. The pre-factor C is determined from the relation $[\mathrm{d}(rg_l)/\mathrm{d}r]_{r'+} - [\mathrm{d}(rg_l)/\mathrm{d}r]_{r'-} = -1/4\pi r'$. It involves a Wronskian $W(J_l, H_l)$ and can be shown to be independent of r', L and L'.

$$g(\boldsymbol{r}_s, \boldsymbol{r}_s', U) = \sum_{LL'} \sum g_{LL'}^n(r_{ns}, E) Y_L(\hat{\boldsymbol{r}}_{ns}) Y_L(\hat{\boldsymbol{r}}_{ns}')$$

$$g_{LL'}^n(r_{ns}, E) = CW(J_l, H_l) Q_{LL'}^{nn}(r_{ns}, E)/H'(r_{ns}, E). \tag{1.11}$$

In case region I contains more than one muffin-tin potential, the boundary may be broken up into sections S_j, $j = 1, 2, \ldots, p$ such that all points on S_j are near the outer muffin-tin potential labelled j. Now, in general,

$$g_{LL'}^{nm}(r_s, r_s, E) = CW(J_l, H_l) Q_{LL'}^{nm}(r_s, E)/H_l'(r_s, E). \tag{1.12}$$

So far our equations have been functional relations. For practical calculations, it is convenient to choose a countable basis of representation. This is very similar to the procedure followed in molecular chemistry. The choice of our basis set $p_i(\boldsymbol{r})$ is dictated by symmetry considerations in a specific problem. Inglesfield, working with flat wells for example, chose the s-like functions $p_i(\boldsymbol{r}) = [\sin(k_i r)/r] Y_{00}(r)$ for the study of s states. Our equations then reduce to matrix equations.

In general, we may represent any operator

$$f(\boldsymbol{r}, \boldsymbol{r}') = \Sigma\Sigma_{LL'} f_{LL'}(r, r') Y_L(\hat{\boldsymbol{r}}) Y_L(\hat{\boldsymbol{r}}')$$

as a matrix

$$f_{ij}^{LL'} = \iint \mathrm{d}r\,\mathrm{d}r'\,(rr')^2 p_{iL}(r) f_{LL'}(r, r') p_{jL'}(r'). \tag{1.13}$$

The effective Hamiltonian operator involves

$$\begin{aligned} h_{LL'}(r, r') &= \delta_{LL'}[\delta(r - r')/r^2][(1/r^2)\,\mathrm{d}^2/\mathrm{d}r^2 + V(r) + l(l+1)/r^2] \\ &\quad + \delta_{LL'}[\delta(r - r_s)/2r_s^2]\mathrm{d}/\mathrm{d}r \\ &\quad \times k_{LL'}(r, r') = [\delta(r - r_s)/r_s^2]k_{LL'}(r_s). \end{aligned} \tag{1.14}$$

Equation (1.6) then reduces to

$$\begin{aligned} G(\boldsymbol{r}, \boldsymbol{r}') &= \sum\sum_{ijLL'}\sum p_{iL}(r) p_{jL'}(r') G_{ij}^{LL'}(r, r', E) Y_L(\hat{r}) Y_{L'}(\hat{r}') \\ &\quad \times (h_{ij}^{LL'} + k_{ij}^{LL'} - E S_{ij}^{LL'}) G_{ij}^{LL'} = \delta_{ij}\delta_{LL'} \end{aligned} \tag{1.15}$$

i.e. $\mathbf{G} = (\mathbf{h} + \mathbf{k} - E\mathbf{S})^{-1}$ where $\mathbf{S}$ is the overlap matrix of the basis set.

The density of states is given by

$$n(E) = \sum\sum_{Lij}\sum S_{ij}^{LL'}\left(-\frac{1}{\pi}\mathrm{Im}[G_{ij}^{LL}(E)]\right). \tag{1.16}$$

The charge density is given by

$$\sum\sum_{ijLL'}\sum p_{iL}(r) p_{jL'}(r) Y_L(r) Y_{L'}(r')\left[-\frac{1}{\pi}\mathrm{Im}\left(\int^{E_F} \mathrm{d}E\, G_{ij}^{LL'}\right)\right]. \tag{1.17}$$

The CPA equation reduces to a set of equations

$$\int \mathrm{d}V\, P(V) G_{ij}^{LL'}(V, u) = G_{ij}^{LL'}(u, u). \tag{1.18}$$

The coherent potential $u(\boldsymbol{r}, E)$ is characterised by the effective inverse scattering matrix $c_n^{LL'}(E)$ which can be obtained from the above equation. $P(V)$ is the distribution of the potentials within region I.

2. Examples and results

We shall illustrate our formalism by simple examples. In the first example, we take $V(\boldsymbol{r}) = -V_A$ or $-V_B$ with probability x_A or x_B in region I and zero outside, i.e. a flat potential. In region II, we have a *coherent jellium* $u(\boldsymbol{r}, E) = u(E)$.

We shall first study the s states in this flat potential. Our basis functions are then $[\sin(nr)]/r$. In this basis,

$$\begin{aligned} h_{nm} &= (n^2/2 - V)S_{nm} + \tfrac{1}{2}\sin(nr_s)\{m\cos(mr_s) - [\sin(mr_s)]/r_s\} \\ k_{nm} &= \sin(nr_s)\sin(mr_s)(1 - \mathrm{i}kr_s)/r_s \qquad k = [2(E - V)]^{1/2} \\ S_{nm} &= \tfrac{1}{2}[\{\sin[(n - m)r_s]\}/(n - m) - \{\sin[(n + m)r_s]\}/(n + m)]. \end{aligned} \tag{2.1}$$

The CPA equations are given by

$$x_A G_{nm}(E, V_A, u_{nm}) + x_B G_{nm}(E, V_B, u_{nm}) = G_{nm}(E, u, u_{nm}). \tag{2.2}$$

The number of members in the basis set $\{p_{nL}(\boldsymbol{r})\}$ $\{n = 1, 2, \ldots, N\}$ varies from problem to problem. In figure 1(*a*) we show the densities of states for $V_A = -1.0$ au,

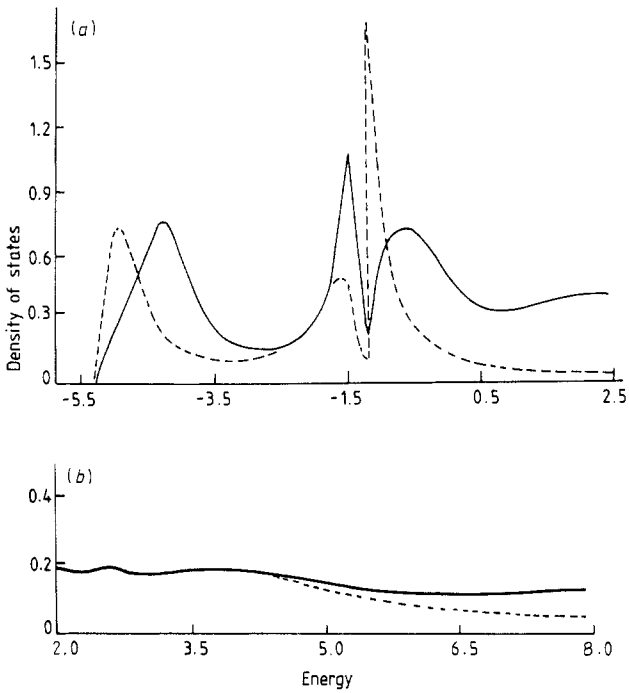

Figure 1. (*a*) Densities of states for $V_A = -1.0$ au, $V_B = -5.0$ au, $r_s = 2$ au and $x_A = x_B = 0.5$: ---, single-member basis; ——, eight-member basis. (*b*) Difference in the densities of states for a four-member basis (----) calculation and an eight-member basis calculation (——) for the same parameters as above with $x_A = 0.9$ and $x_B = 0.1$ at higher energies.

$V_B = -5.0$ au, $r_s = 2$ au, $x_A = x_B = 0.5$. The broken curve is obtained for $n = 1$ and the full curve for $n = 8$. The essential qualitative features are already reproduced for $n = 1$, whereas increasing n leads to shifts in the peaks as well as in the broadening. Essential differences occur at higher energies. Figure 1(*b*) shows a result for the same potentials but for concentration $x_A = 0.9$ and $x_B = 0.1$ at higher-energy regimes for $n = 4$ (broken curve) and $n = 8$ (full curve). The two differ very little except at very high energies and even then the ratio of the difference to the average peak height is only about 4%.

To illustrate the effects of concentration and $|V_A - V_B|$ (the two parameters characterising disordered alloys), we show in figure 2 three sets of alloys for $n = 1$ (broken curves) and $n = 8$ (full curves) and $x_A = 0.3$, 0.5 and 0.7.

Figure 2(*a*) is for $V_B = -1.0$ au and $V_A = -0.5$ au. This is the overlapping-band weak-disorder case. The peaks corresponding to the constituents overlap to form a broad structure; the relative weights of each constituent are reflected in the concentrations.

Figure 2(*b*) is for $V_B = -5.0$ au and $V_A = -1.0$ au. This is the *split-band* strong-scattering regime. Each constituent contributes distinguishable structures whose weights again are reflected in the concentrations.

Figure 2(*c*) is for $V_B = -5.0$ au and $V_A = -0.5$ au and $x_A = 0.1$ and 0.9. This is the so-called *impurity band* strong-scattering regime. It is here that, from our experience with tight-binding calculations, cluster effects (not reflected in the CPA calculation here) are expected to dominate.

We shall now look at the density of states for d-like states in the flat potential. The

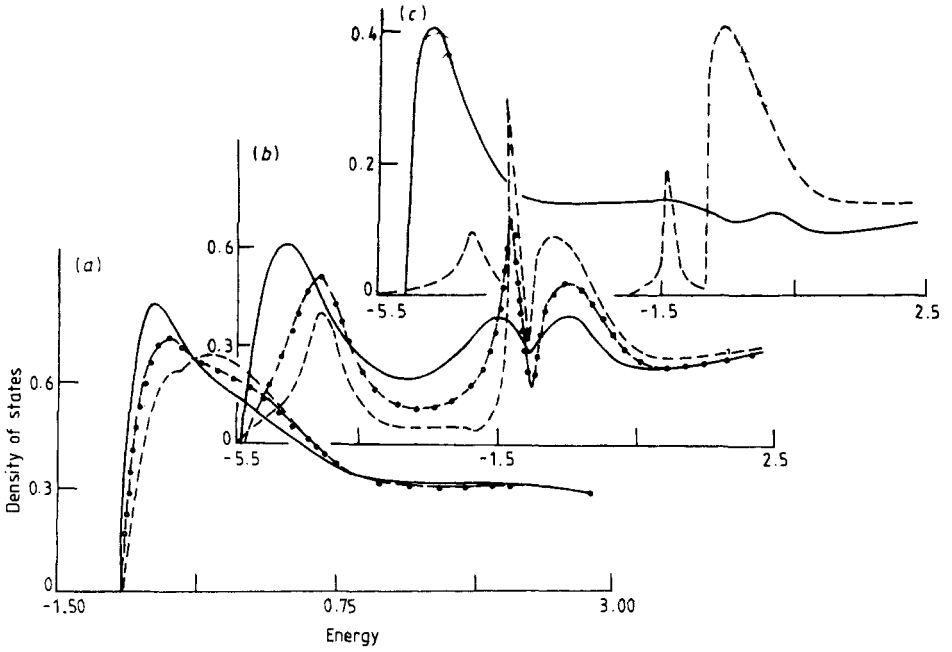

Figure 2. Densities of states for s states in a flat potential binary alloy with (*a*) $V_B = -1.0$ au and $V_A = -0.5$ au, (*b*) $V_B = -5.0$ au and $V_A = -1.0$ au and (*c*) $V_B = -5.0$ au and $V_A = -0.5$ au. For (*a*) and (*b*): --- $x_A = 0.3$; —·— $x_A = 0.5$; —— $x_A = 0.7$; for (*c*): --- $x_A = 0.1$; —— $x_A = 0.9$.

basis states are now $[(3/p^3 - 1/p)\sin p - (3/p^2)\cos p]Y_{22}(r)$ where $p = nr$. We shall deal only with single-member basis with $n = 1$. The d states are far less extended than the s states and the qualitative results are better reflected in the simple $n = 1$ case than for the s-like states. The representation of the Hamiltonian is then

$$h_{nn} = (n^2/2 - V)S_{nn} + \tfrac{1}{2}\{[2/nr_s + 3/(nr_s)^3 - 27/(nr_s)^5]\sin^2(nr_s)]/n + [1 - 6/(nr_s)^2 + 54/(nr_s)^4][\sin(2nr_s)]/2n + [3/nr_s + 9/(nr_s)^3][\cos^2(nr_s)]/n\}$$

$$S_{nn} = (1/2n^2)\{r_s - [\sin(2nr_s)]/2n\} + \tfrac{3}{2}[\cos(2nr_s)]/n^6r_s^3 - \tfrac{3}{2}[\cos(2nr_s)]/n^4r_s - [3\sin(2nr_s)]/n^5r_s^2 - 3/[2n^4r_s - 3/2n^6r_s^3]$$

$$k_{nn} = \tfrac{1}{2}[(9/n^6r_s^5 + 1/n^2r_s - 6/n^4r_s^3)\sin^2(nr_s) + [9\cos^2(nr_s)]/n^4r_s^3 - (3/n^2)(3/n^3r_s^4 - 1/nr_s^2)\sin(2nr_s)] \times [(9 - 9ikr_s - 4k^2r_s^2 + ik^3r_s^3)/(3 - 3ikr_s - k^2r_s^2)]. \quad (2.3)$$

Figures 3(*a*)–3(*c*) shows the d-state density of states for the corresponding parameters of the s states shown in the earlier figures. The structures are sharper. This is to be expected since the d states fall away more sharply from the well centres than do the s states. The qualitative features are well reproduced by the single-member basis.

To study the effect of the well shape, we next carry out a similar calculation for a $1/r$ type of potential. We shall look at the s-like states in the $1/r$ potential. The basis is made up of functions such as $2n^{3/2}\exp(-nr)$. Again we shall first look at a basis with

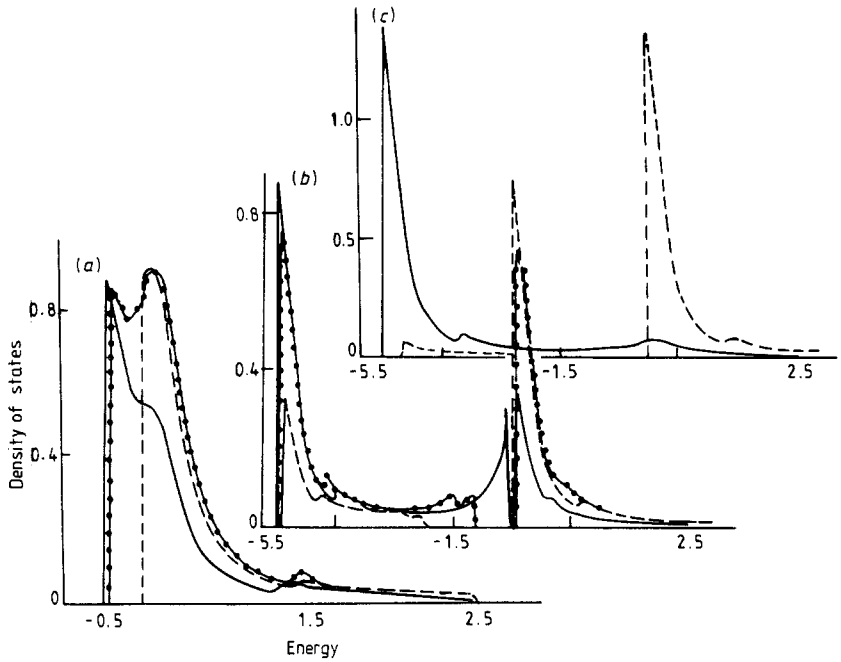

Figure 3. Densities of states for the d states in a flat potential binary alloy with the same parameters as the corresponding parts in figure 2.

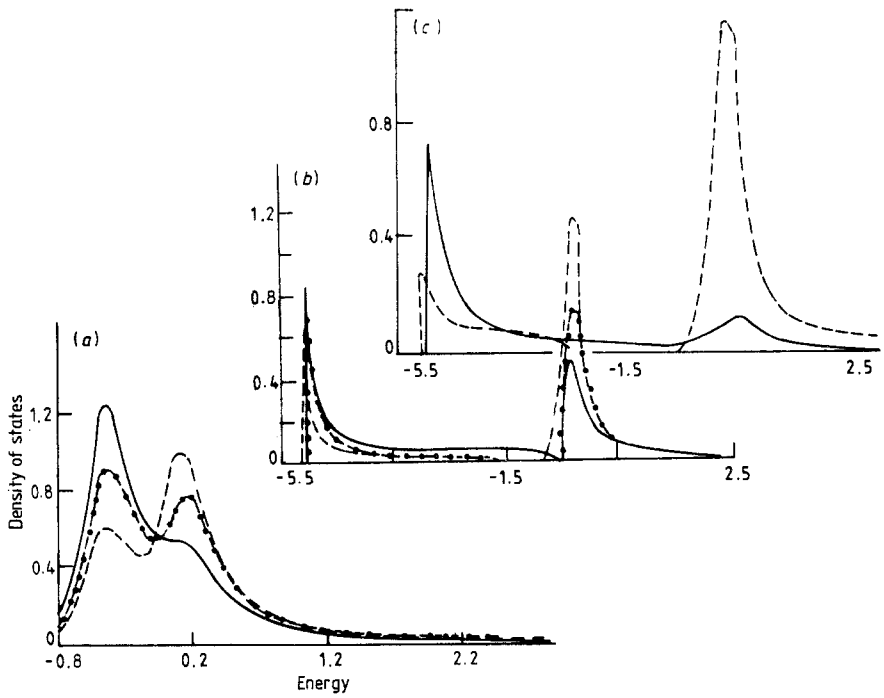

Figure 4. Densities of states for the s states in a binary alloy with potentials of the form $V(r) = V/r$, with V taking the values V_A and V_B with probabilities x_A and x_B. The parameters are the same as in the corresponding parts in figures 2 and 3.

only $n = 1$. The Hamiltonian representation is given by

$$h_{nn} = -(n^2/2)S_{nn} + 4(n - V)n^3\{[-(1/2n)^2 - r_s/n]\exp(-2nr_s) + (1/2n)^2\} - 2n^4 r_s^2 \exp(-2nr_s)$$

$$k_{nn} = (n^3 r_s/2)\exp(-2nr_s)(1 - ikr_s)$$

$$S_{nn} = 4n^3[(-r_s^2/2n - 2r_s/2n^2 - 2/2n^3)\exp(-2nr_s) + 2/2n^3]. \tag{2.4}$$

Figure 4 shows the effect of the well shape. We have taken the two potentials to be $V(r) = V/r$ where V can be either V_A or V_B. The qualitative features remain unchanged from the flat potentials, although the quantitative change in the location and the widths of the structures are apparent. The structures are sharper than the flat potentials, which is a reflection of the fact that the flat well s states increase as $1/r$ whereas the $1/r$ potential wavefunction decays exponentially. The density of states also correspondingly decay at higher energies, and the peak widths are narrower.

The formalism is ideally suited to extension of the CCPA. We may embed a cluster of muffin-tin potentials within the spherical region I (as in figure 5). The matrix representation of the Hamiltonian will then be in terms of a basis centred at each of the wells. This is reminiscent of the type of approach used in molecular electronic structure calculations with an atomic-like basis. The calculations will then involve multi-centre integrals. Apart from this complication, which has already been dealt with in great detail in molecular calculations, the rest of the procedure follows as described earlier. Work on the CCPA using the embedding method is in progress and the subsequent calculation will be reported.

Appendix

By definition the functional inverse of the Green function is

$$\int d^3\boldsymbol{r}''\, k(\boldsymbol{r}, \boldsymbol{r}'')g(\boldsymbol{r}'', \boldsymbol{r}') = \delta^3(\boldsymbol{r} - \boldsymbol{r}').$$

Expanding $k(\boldsymbol{r}, \boldsymbol{r}'')$ and $\delta^3(\boldsymbol{r} - \boldsymbol{r}')$ in the forms $k(\boldsymbol{r}, \boldsymbol{r}'') = \Sigma_L k_l(r, r'')Y_L(r)Y_L(r'')$ and $\delta^3(\boldsymbol{r} - \boldsymbol{r}') = (1/r^2)\delta(r - r')\Sigma_L V_L(r)Y_L(r')$, substituting into the above equations and equating coefficients of $Y_L(r)Y_L(r')$ on either side, we get

$$\int dr''\, r''^2 k_l(r, r'')g_l(r'', r') = \frac{1}{r^2}\delta(r - r').$$

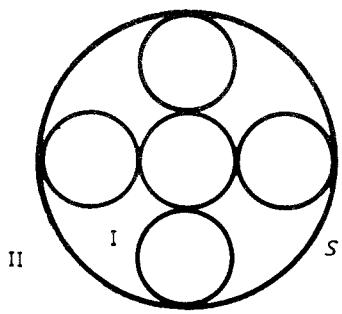

Figure 5. A schematic diagram showing a cluster of spherically symmetric wells with a modified spherical boundary.

Note from the form of k that $k_l(r, r'') = \delta(r'' - r_s)k(r, r_s)$ so that, if we put both r and $r' = r_s$, we obtain from the above

$$k_l(r_s) = (1/r_s)^4 g_l(r_s).$$

References

Faulkner J S and Stocks G M 1980 *Phys. Rev.* B **21** 3222
Gonis A, Stocks G M, Butler W H and Winter H 1984 *Phys. Rev.* B **29** 555
Gray L J and Kaplan T 1976a *J. Phys. C: Solid State Phys.* **15** L303, L483
—— 1976b *Phys. Rev.* B **14** 3462
Inglesfield J E 1971 *J. Phys. C: Solid State Phys.* **4** L14
—— 1972 *J. Phys. F: Met. Phys.* **2** 878
—— 1981 *J. Phys. C: Solid State Phys.* **14** 3795
Kumar V, Mookerjee A and Srivastava V K 1982 *J. Phys. C: Solid State Phys.* **15** 1939
Mookerjee A 1973 *J. Phys. C: Solid State Phys.* **6** L205, 1340
—— 1987 *J. Phys. F: Met. Phys.* **17** 1511